P4.12 Dust detection and quantification from MODIS IR bands using Artificial Neural Network (ANN) model

Sang-Sam Lee and Byung-Ju Sohn*
School of Earth and Environmental Sciences, Seoul National University, Seoul, 151-747, KOREA

1. Introduction

Asian dust is a typical example of mineral aerosol originating in the Gobi desert, Sand desert, Loess plateau, and barren mixed soil in northern China and Mongolia during the spring season in most cases (Chun *et al.*, 2001; In and Park, 2002; Park and In, 2003, Lee *et al.*, 2005). Recently, more intense and frequent dust storms in East Asia have increased with the gradual expansion in arid desertification owing to heavy cultivation, overgrazing, and lack of precipitation in the source regions (Chun and Lim, 2004).

In recent decades, the geographical origin and temporal variability of the Asian dust have been studied using various field measurements, meteorological analysis, and satellite observations (Uematsu *et al.*, 1983; Lee *et al.*, 2002; Kim *et al.*, 2004; Nakajima *et al.*, 2007). Among them, satellite observations have been a useful tool for monitoring the amount and transportation of Asian dust due to its broad geographical coverage including oceanic area. Remote sensed retrieval techniques of aerosol using visible and near-infrared bands have been developed for many years but have a limitation over bright surfaces and at nighttime. Thus, it is expected to use IR bands for remote sensing of aerosol because they can monitor continuously, both day and night. With this advantage, there have been several efforts to derive the detection and quantification method of dust from satellite measurement using IR bands (Shenk and Curran, 1974; Ackerman, 1997; Wald *et al.*, 1998; Sokolik, 2002). However these conclusions are not allowed to determine aerosol optical properties such as the aerosol optical depth (AOD) or the Angstrom exponent but a relative dust index or threshold value for detection of dust. The purpose of this study is to retrieve the AOD of dust over East Asian region at day and night from Moderate-Resolution Imaging Spectrometer (MODIS) using IR bands.

2. Data

2.1 MODIS

MODIS Aqua data are analyzed to use the brightness temperatures, AOD, and land cover on East Asia domain (20°N-55°N, 90°E-145°E) in spring (March - May) of 2006 - 2007.

Brightness temperature data were inverted from MODIS Level 1B calibrated radiance with a 1km resolution using inverse of the Planck function with sensor response functions. AOD at 550 nm wavelength was selected from MYD04_L2 product of “Deep Blue Aerosol Optical Depth 550 Land” over land and “Optical Depth Land And Ocean” over ocean, respectively. Land cover was obtained from MYD12_Q1 product of “IGBP Land Cover Type” including 17 classes of land cover in the International Geosphere-Biosphere Programme (IGBP) global vegetation classification scheme.

2.2 AERONET

To match with MODIS brightness temperature data we use ground based sun/sky radiation measurements of AERONET level 2.0 data at the same domain and time. Total 38 sites were selected and AOD at 550nm were interpolated from AOD (440) and Angstrom exponent α (440 - 675 nm) by

$$AOD(550nm) = \left[AOD(440nm) \Big/ \left(\frac{550nm}{440nm} \right)^{\alpha(440-675)} \right] \quad (1)$$

.

These interpolated AERONET AOD at 550nm are selected with spatio-temporal constraints that the MODIS pixels are located within ± 0.1 deg from the AERONET site and measured within ± 30 minutes compared with AERONET measurement. Consequently, we can collect the 583 datasets over East Asia domain in the spring of 2006 - 2007.

2.3 Topography and Emissivity

Topography data are based on the 1 km averages derived from the USGS SRTM30 grided DEM data product created with data from the NASA Shuttle Radar Topography Mission. GTOPO30 data are used for high latitude where SRTM data are not available (see online at http://topex.ucsd.edu/).

ASTER emissivity spectra ranged from 3.5 to 14 ㎛ of 9 samples were used to characterize the 17 IGBP surface types (Table 1). The ASTER spectral library includes data from three other spectral libraries: the Johns Hopkins University (JHU) Spectral Library, the Jet Propulsion Laboratory (JPL) Spectral Library, and the United States Geological Survey (USGS – Reston) Spectral Library (see online at http://speclib.jpl.nasa.gov/). Spectral emissivities are weighted and averaged along

*Corresponding author address: Byung-Ju Sohn, School of Earth and Environmental Sciences, Seoul National University, NS80, Seoul, 151-747, KOREA
E-mail: sohn@snu.ac.kr

each wavelength interval of the MODIS band with known response function for each IGBP surface type. Because temperature dependence of the emissivity is usually very small for most surface materials, the band-average emissivities in MODIS IR bands are defiend by

$$\overline{\varepsilon_i} = \frac{\int_{\lambda(i,lower)}^{\lambda(i,upper)} \varepsilon_\lambda r_\lambda d\lambda}{\int_{\lambda(i,lower)}^{\lambda(i,upper)} r_\lambda d\lambda} \quad (2)$$

where ε_λ is the spectral emissivity from ASTER spectral library for each IGBP type from Table 1 and r_λ is the response function of MODIS in band i.

Table 1. Assignment of laboratory measurements to surface types [Adapted from Wilber *et al.*, 1999].

Type ID	IGBP type	Spectral library
1	Evergreen Needleleaf Forest	Conifer
2	Evergreen Broadleaf Forest	Conifer
3	Deciduous Needleleaf Forest	Deciduous
4	Deciduous Broadleaf Forest	Deciduous
5	Mixed Forest	1/2 Conifer + 1/2 Deciduous
6	Closed Shrublands	1/4 Quartz sand + 3/8 Conifer + 3/8 Deciduous
7	Open Shrubland	3/4 Quartz sand + 1/8 Conifer + 1/8 Deciduous
8	Woody Savannas	Grass
9	Savannas	Grass
10	Grasslands	Grass
11	Permanent Wetlands	1/2 Grass + 1/2 Seawater
12	Croplands	Grass
13	Urban	Black Body
14	Cropland/Mosaic	1/2 Grass + 1/4 Conifer + 1/4 Deciduous
15	Snow and Ice	Mean Of Fine, Medium, and Coarse snow and Ice
16	Barren	Quartz sand
17	Water Bodies	Seawater
18	Tundra	Frost

3. Method

3.1 Artificial Neural Network (ANN)

Artificial Neural Network (ANN) method is recognized as a good tool for modeling inverse problems in geophysical applications (Thiria *et al.*, 1993; Chevallier *et al.*, 1998; Jamet *et al.*, 2004; Gan *et al.*, 2004; Niang *et al.*, 2006; Beal *et al.*, 2007). We use a ANN model, the so-called MLP (Multi-Layer Perceptron) allowing a feed-forward backpropagation to retrieve aerosol optical depth at 550nm from MODIS measurements of brightness temperatures in the IR bands. The architecture of ANN made of 29 inputs, the 12 MODIS brightness temperatures (from band 24 to band 36, except for band 26), '$TB_{11\mu m}$ - $TB_{12\mu m}$', 13 surface emissivities (from band 20 to band 33, except for band 26), surface temperature (Land : Price (1984) Algorithm, Sea : The IMAPP MODIS SST Algorithm (see online at: ftp://ftp.ssec.wisc.edu/pub/IMAPP/MODIS/Level-2/v1.5/SST_DOC.pdf)), relative airmass from surface to sensor ($\sec\theta_{sen}$; θ_{sen} is a sensor zenith angle), and topography. The target output is the AOD at 550nm from AERONET and MODIS at land and ocean, respectively. The ANN model has a single hidden

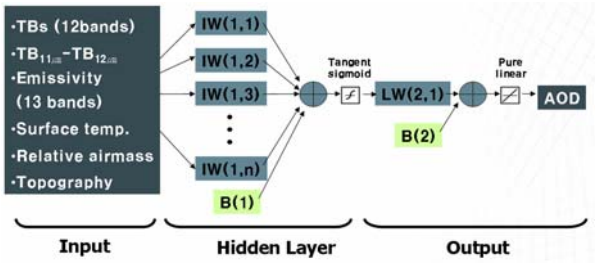

Figure 1. The architecture of the ANN showing 29 inputs, single hidden layer with *n* neurons, and a target output.

layer between inputs and target output, and the nonlinear response of a neuron to its inputs, due to the tangent sigmoidal function, allows for the nonlinear fitting of the function parameterized by the neural network in this study (Figure 1). In the training procedure 10 and 20 neurons provided the best performances for land and ocean, respectively. The optimal learning rate was 0.1 for the both ANN models.

4. Result and Discussion

Aerosol optical depth has been retrieved using artificial neural network (ANN) method from AERONET and MODIS Aqua data. Cloud screen process by IR bands is carried out based on MODIS BTD cloud mask algorithm (Ackerman *et al.*, 2006). To validate the ANN results we compare the ANN retrievals and MODIS AOD at daytime. In Figure 2, correlation coefficient between ANN model result and MODIS AOD was found to be 0.79 on 0440UTC 8 April 2006 which was one of the heaviest outbreak cases in the spring of 2006 - 2007. Also noted is that the aerosols whose optical depth is less (greater) than 1.0 tend to overestimation (underestimation) and those whose optical depth is greater than 2.5 are inverted

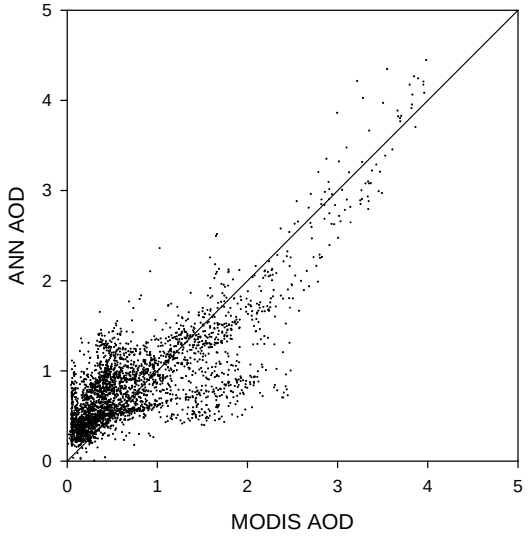

Figure 2. Comparison between MODIS AOD and ANN AOD trained with AERONET data (Land) and MODIS data (Ocean) at 0440UTC 8 April 2006.

(a)

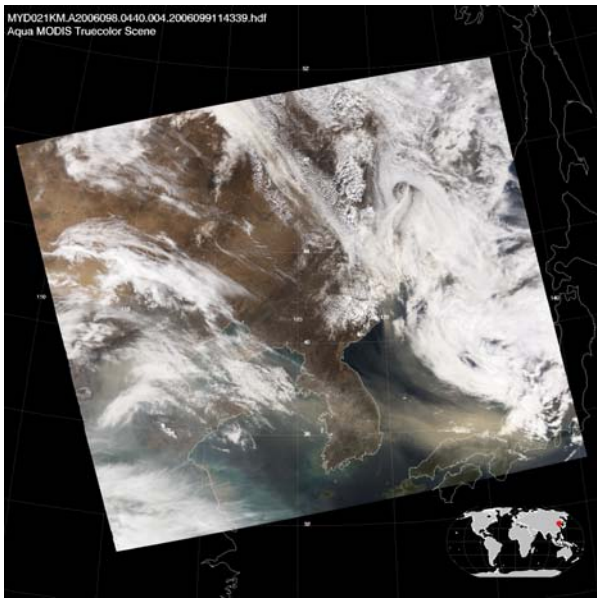

(b)

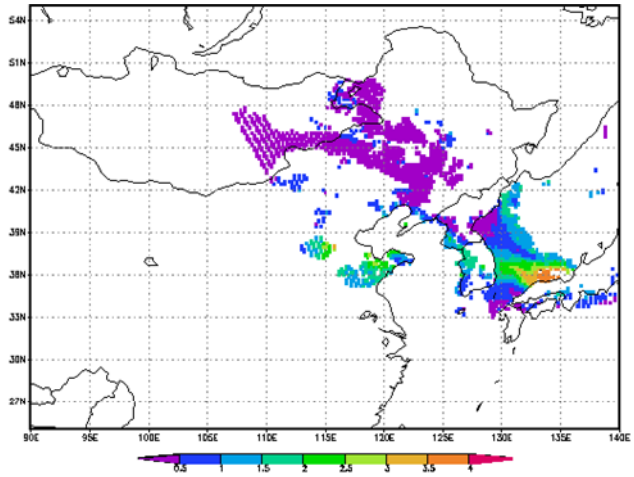

(c)

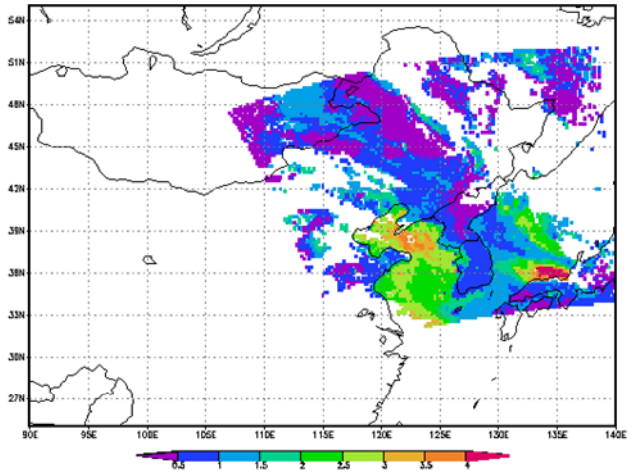

Figure 3. (a) True color composite over Korean peninsula, (b) MODIS AOD (Land: Deep blue algorithm), (c) ANN AOD trained with AERONET data (Land) and MODIS data (Ocean) at 0440UTC 8 April 2006. The MODIS BTD cloud mask algorithm is used.

very well from ANN model comparing with MODIS AOD. In other words, ANN model have a capability to retrieve the optical properties of dust having large AOD. However, the retrieval of aerosols having small AOD from ANN model shows problematic aspect due to the lack of aerosol type classification algorithm.

Figure 3 shows true color composite and spatial distribution of ANN and MODIS AOD at the same time. In the MODIS BTD cloud mask algorithm, because threshold for optically thin cirrus detection is function of total precipitable water it has a limitation to mask cirrus cloud from brightness temperature only (Ackerman, 2006). For this reason the cirrus above the West Sea of Korean peninsula cannot be masked in our algorithm. With exception this problem, spatial distribution of AOD retrieved from ANN is agreed well with MODIS AOD.

In this study we showed ANN model has a good potential to retrieve aerosol optical depth. More examinations and trials are need, however, to improve this ANN algorithm using IR bands. Also this model should be extended to specify the dust aerosol property from other aerosols and clouds to assure that it has a capability both day and night.

Acknowledgment

This work was supported by the Korea Research Foundation Grant funded by the Korean Government (MOEHRD) KRF-2007-511-C00078; and the Korea Meteorological Administration Research and Development Program under grant CATER 2006-2103. We thank the AERONET Principal Investigators (Tanre´ D., Holben B., Guyon D., Mitchell R., Karmer O., Ruddick K., Verbrugghe M. and Francois C.) and their staff for establishing and maintaining the 38 sites used in this investigation.

References

Ackerman, S. A., 1997: Remote sensing aerosols using satellite infrared observations, *J. Geophys. Res.*, **102**, 17,069– 17,080.

Ackerman, S. A., K. I. Strabala, W. P. Menzel, R. A. Frey, C. C. Moeller, and L. E. Gumley, B. Baum, S. W. Seemann, and H. Zhang, 2006: Discriminating Clear-Sky from Cloud with MODIS – Algorithm Theoretical Basis Document. Products: MOD35_L2 ATBD Reference Number: ATBD-MOD-06.

Beal, D., F. Baret, C. Bacour, and X-F. Gu, 2007: A method for aerosol correction from the spectral variation in the visible and near infrared: application to the MERIS sensor, *International Journal of Remote Sensing*, **28**(3), 761 – 779.

Chevallier,F., F. Cheruy, N.A. Scott, and A. Chedin, 1998: A neural network approach for a fast and accurate computation of longwave radiative budget, *J. Appl. Meteor.*, **37**, 1385-1397.

Chun, Y., J. Kim, J.C. Choi, K.O. Boo, S.N. Oh, and M. Lee, 2001: Characteristic number size distribution

of aerosol during Asian dust period in Korea. *Atmospheric Environment*, **35**, 2715–2721.

_____, J.Y. Lim, 2004. The recent characteristics of Asian Dust and Haze events in Seoul, Korea. *Meteorology and Atmospheric Physics*, **87**, 143–152.

Gan, T.Y., Kalinga, O., K. Ohgushi, and H. Araki, 2004: Retrieving Seawater Turbidity From Landsat-TM Data by Regressions and Artificial Neural Network, *Int. J. Remote Sensing*, **25**(21), 4593-4615.

In, H.-J., and S.-U. Park, 2002: A simulation of longrange transport of Yellow Sand observed in April 1998 in Korea. *Atmospheric Environment*, **36**, 4173–4187.

Jamet, C., C. Moulin, and S. Thiria (2004), Monitoring aerosol optical properties over the Mediterranean from SeaWiFS images using a neural network inversion, *Geophys. Res. Lett.*, **31**, L13107, doi:10.1029/2004GL019951.

Kim, D.-H., B.-J. Sohn, T. Nakajima, T. Takamura, T. Takemura, B.-C. Choi, and S.-C. Yoon, 2004: Aerosol optical properties over east Asia determined from ground-based sky radiation measurements, *J. Geophys. Res.*, **109**, D02209, doi:10.1029/2003JD003387.

Lee. S.-S., B.-J. Sohn, D.-S. Shin, H. Fukushima, and T. Nakajima, 2002: Optical Characteristics of the Asian Dust Aerosol from Sky Radiation Measurements in Spring 1998, Korean *J. Atmos. Sci.*, **5**(2), 161-170.

Lee, S.-S., Y. Chun, J.-C. Nam, S.-U. Park, and E.-H. Lee, 2005: Estimation of Dry Deposition during Asian Dust Events in Spring of 2002, *J. Meteor. Soc. Japan*, **83**A, 241-254.

Nakajima, T., *et al.*, 2007: Overview of the Atmospheric Brown Cloud East Asian Regional Experiment 2005 and a study of the aerosol direct radiative forcing in east Asia, *J. Geophys. Res.*, **112**, D24S91, doi:10.1029/2007JD009009.

Niang, A., F. Badran, C. Moulin, M. Crepon, and S. Thiria, 2006: Retrieval of aerosol type and optical thickness over the Mediterranean from SeaWiFS images using an automatic neural classification method, *Remote Sensing of Environment*, **100**, 82-94.

Park, S.-U., and H.-J. In, 2003. Parameterization of dust emission for the simulation of the Yellow Sand (Asian dust) observed in March 2002 in Korea. Journal of Geophysical Research 108 (D19), 4618 (doi:10.1029/2003JD003484).

Price, J. C., 1984: Land surface temperature measurements from the split window channels of the NOAA-7 Advanced Very High Resolution Radiometer, *Journal of Geophysical Research*, **89**, 7231-3237.

Shenk, W.E. and R.J. Curran, 1973: The detection of dust storms over land and water with satellite visible and infrared measurements, *Mon. Weather Rev.*, **102**, 830-837.

Sokolik, I. N., 2002: The spectral radiative signature of wind-blown mineral dust: Implications for remote sensing in the thermal IR region, *Geophys. Res. Lett.*, **29**(24), 2154, doi:10.1029/2002GL015910.

Thiria, S., C. Mejia, F. Badran, and M. Crepon, 1993: A neural network approach for modeling nonlinear transfer functions: Application for wind retrieval from spaceborne scatterometer data, *J. Geophys. Res.*, **98**, 2827– 2842.

Uematsu, M., R. Duce, J.M. Prospero, L. Chen, and J.T. Merrill, and R.L. McDonald, 1983: Transport of mineral aerosol from Asia over the North Pacific ocean, *J. Geophys. Res.*, **88**, 5343-5352.

Wald, A.E., Y.J. Kaufman, D. Tanre, and B.-C. Gao, 1998: Daytime and nighttime detection of mineral dust over desert using infrared spectral contrast, *J. Geophys. Res.*, **103**, 32307-32313.

Wilber, A.C., D.P. Kratz, and S.K. Gupta, 1999: Surface emissivity maps for use in satellite retrievals of longwave radiation. *NASA Tech. Rep.* NASA/TP-1999–209362, NASA, 30 pp.